Published in final edited form as:

ACS Chem Neurosci. 2021 February 03; 12(3): 542–556. doi:10.1021/acschemneuro.0c00755.

Discovery of Molecular Interactions of the Human Melanocortin-4 Receptor (hMC4R) Asp189 (D189) Amino Acid with the Endogenous G-Protein-Coupled Receptor (GPCR) Antagonist Agouti-Related Protein (AGRP) Provides Insights to AGRP's Inverse Agonist Pharmacology at the hMC4R

Mark D. Ericson[1], **Erica M. Haslach**[2], **Sathya M. Schnell**[1], **Katie T. Freeman**[1], **Zhimin M. Xiang**[2], **Frederico P. Portillo**[2], **Robert Speth**[3,4], **Sally A. Litherland**[5], **Carrie Haskell-Luevano**[1,2]

[1]Department of Medicinal Chemistry and Institute for Translational Neuroscience, University of Minnesota, Minneapolis, MN 55455, United States

[2]Departments of Pharmacodynamics and Medicinal Chemistry, University of Florida, Gainesville, FL, 32610, United States

[3]College of Pharmacy, Nova Southeastern University, Fort Lauderdale, FL 33328, United States

[4]College of Medicine, Georgetown University, Washington, D.C. 20057, United States

[5]Translational Research, Florida Hospital Cancer Institute, Orlando, FL, USA

Abstract

The melanocortin receptors (MCRs) are important for numerous biological pathways, including feeding behavior and energy homeostasis. In addition to endogenous peptide agonists, this receptor family has two naturally occurring endogenous antagonists, agouti and agouti-related protein (AGRP). At the melanocortin-4 receptor (MC4R), the AGRP ligand functions as an endogenous inverse agonist in the absence of agonist and as a competitive antagonist in the presence of agonist. At the melanocortin-3 receptor (MC3R), AGRP functions solely as a competitive antagonist in the presence of agonist. The molecular interactions that differentiate AGRP's inverse agonist activity at the MC4R have remained elusive, until the findings reported herein. Based upon homology molecular modeling approaches, we previously postulated a unique interaction between the D189 position of the hMC4R and Asn114 of AGRP. To further test this hypothesis, six D189 mutant hMC4Rs (D189A, D189E, D189N, D189Q, D189S, and D189K) were generated and pharmacologically characterized resulting in the discovery of differences in

Materials & Correspondence chaskell@umn.edu; Phone: 612-626-9262; Fax: 612-626-3114; Street Address: Department of Medicinal Chemistry, University of Minnesota, 308 Harvard Street SE, Minneapolis, MN, 55455, USA.

Author Contributions

M.D.E. and designed and synthesized the macrocyclic peptide library with the help of C.H.-L. Cellular assays and hMC4R receptor mutagenesis experiments were performed by E.M.H., Z.M.X., F.P.P, S.M.S., K.T.F., and S.A.L. R.S. prepared and purified the iodinated peptides. M.D.E. wrote the manuscript with the assistance of C.H.-L.

Supporting Information

Analytical characterization of peptide macrocycles; cDNA sequence of the hMC4R; primer sequences used to generate D189 mutant hMC4Rs.

inverse agonist activity of AGRP and an 11 macrocyclic compound library. These data support the hypothesized interaction between the hMC4R D189 position and Asn114 residue of AGRP and define critical ligand-receptor molecular interactions responsible for the inverse agonist activity of AGRP at the hMC4R.

Graphical Abstract

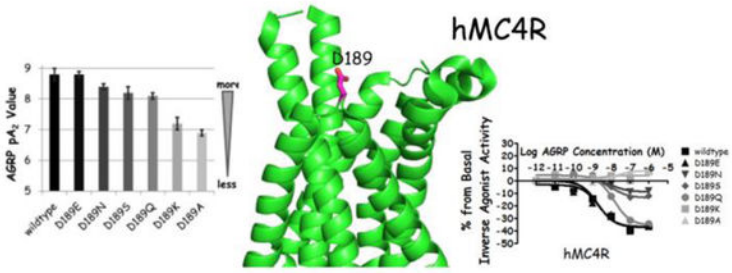

Keywords

macrocyclic peptide; mutant hMC4R; inverse agonism

Introduction

The melanocortin system has been associated with many physiological functions, including skin pigmentation,[1–2] steroidogenesis,[3] and energy homeostasis.[4] Five melanocortin receptors have been identified to date that are members of the super-family of G protein-coupled receptors (GPCRs).[5–13] The melanocortin receptors couple to $G_{\alpha s}$ protein subunits and increase intracellular levels of cAMP following agonist stimulation.[14] Naturally occurring ligands for the receptors include peptide agonists derived from the proopiomelanocortin (POMC) gene transcript[15] and two endogenous antagonists, agouti[16–18] and agouti-related protein (AGRP).[19–21] In addition to antagonist pharmacology at the centrally expressed melanocortin-3 receptor (MC3R) and melanocortin-4 receptor (MC4R), AGRP has also been reported to possess inverse agonist activity at the MC4R in the absence of agonist.[22–23] Both the MC3R and MC4R have been implicated in food intake and energy homeostasis.[4, 24–25] Intracerebroventricular (ICV) administration of agonists to the MC3R and MC4R decreased food intake in rodents,[24–27] while antagonists increased food intake.[24–25, 28] Single nucleotide polymorphisms within the human MC4R have been directly linked to an obese phenotype.[29–30] These data suggest developing new compounds that modulate the centrally expressed melanocortin receptors may result in novel therapies for weight management, for conditions of both positive energy balance including obesity and negative energy balance such as cachexia and anorexia.

Since the sequence of α-MSH (a naturally occurring agonist ligand from the POMC gene transcript) was first reported in 1957,[31] numerous melanocortin ligands have been developed based upon this peptide. However, not many melanocortin ligands have been developed from AGRP, perhaps in part because AGRP was first reported 40 years following α-MSH,[19–21] the large size of the proposed active form of AGRP *in vivo* (50 residues versus 13 residues in

α-MSH),[32] and the structural complexity of AGRP indicated by NMR studies (10 cysteine residues forming 5 disulfide bridges).[33–34] Many truncated forms of AGRP also possess decreased antagonist potency.[35–37] One previously identified macrocyclic octapeptide scaffold, based upon the postulated active loop domain of AGRP, cyclized head-to-tail through a DPro-Pro motif (c[Pro-Arg-Phe-Phe-Asn-Ala-Phe-DPro] representing the Arg111-Phe116 residues of AGRP) was 50-fold less potent at the mouse (m)MC4R (and 300-fold at the mMC3R) compared to AGRP.[38] Further structure-activity relationship (SAR) studies replacing the Asn114 with a diaminopropionic (Dap) acid residue resulted in an equipotent antagonist to AGRP at the mMC4R.[38] Additional SAR studies reported Dap, DDap, and His residues at the Asn114 position,[39] Ser at the Ala115 position,[39] and Ala, Nle, Trp, and Tyr at the Phe116 position[39–40] maintained mMC4R antagonist potency, as did incorporating peptoid residues at the Phe113 and Asn114 positions.[41] Incorporating multiple of the substitutions described above into the DPro-Pro macrocyclic scaffold resulted in ligands that were up to 6-fold more potent than AGRP at the mMC4R, and over 600-fold selective for the mMC4R compared to the mMC3R.[42] Replacement of the postulated AGRP Arg-Phe-Phe antagonist pharmacophore with the agonist His-DPhe-Arg-Trp tetrapeptide sequence resulted in nanomolar potent mMC4R agonists.[43] Thus potent mMC4R agonists and antagonists have been developed from the AGRP-derived macrocyclic scaffold, which may represent potential lead ligands in the development of novel weight management therapies.

As a translational step in the development of AGRP-derived macrocycles, 11 compounds substituted at the Asn114 position were assessed at the human (h)MC4R, examining antagonist potency, binding affinity, and effects on inverse agonism. Additionally, based upon GPCR homology molecular modeling, we have postulated that the D189 position of the hMC4R is uniquely involved with the Asn114 of AGRP, versus other melanocortin ligands.[44] To further test these hypotheses, a set of six D189 hMC4R mutant receptors were generated and pharmacologically characterized with a panel of known synthetic and endogenous ligands, and probed for functional effects on antagonist potency and inverse agonism with nine of the macrocyclic ligands.

Results and Discussion

Experimental Rationale:

Previously, the AGRP-derived macrocyclic scaffold was examined at the mouse melanocortin receptors.[38–40, 42–43] While many ligands possess similar activities at orthologous mouse and human melanocortin receptors, species differences have been reported, including γ_2-MSH agonist potency at the MC5R.[45] To identify potential species variations with the macrocyclic scaffold at the MC4R, 11 macrocycles substituted at the Asn position (equivalent to the Asn114 position in AGRP) were pharmacologically characterized at the hMC4R. Previous SAR studies at the mMC4R reported basic residues increased antagonist potency relative to the native Asn.[38–39] Therefore Dap (MDE3–119-8c), DDap (MDE3–119-7c), and His (MDE3–119-12c) substitutions were included (Fig. 1a). Polar residue substitutions decreased antagonist potency less than 10-fold compared to the Dap substitution at the mMC4R.[39] Therefore, ligands possessing the native Asn (MDE5–

108-10c) and Ser (MDE3–85c) were examined. Also included were the short, aliphatic Ala (MDE3–154c) and Abu (MDE3–119-2c) residues and the branched aliphatic Val (MDE3–119-10c) residue, which decreased antagonist potencies 24-, 25-, and 630-fold, respectively, compared to the Dap substitution at the mMC4R.[39] The acidic Asp (MDE3–119-4c) and Glu (MDE3–119-5c) amino acids and aromatic Phe (MDE3–119-14c) residue were also examined, which previously decreased antagonist potency 50–100 fold at the mMC4R.[39] All peptides were synthesized, purified to greater than 95%, and characterized by analytical RP-HPLC and MALDI-MS (Supplemental Table 1) as previously described.[39] Compounds were assayed for antagonist activity using a dose-response Schild paradigm[46] and NDP-MSH as the agonist with HEK293 cells stably expressing the hMC4R using the AlphaScreen cAMP assay. In our laboratory, we consider compounds within a 3-fold potency range as equipotent due to the inherent experimental error of the assays across multiple laboratories.

AlphaScreen cAMP Assay at the hMC4R:

The hAGRP(86–132) and the Dap-substituted macrocycle MDE3–119-8c possessed similar nanomolar antagonist potencies at the hMC4R (Fig. 1b and 1c, Table 1). Inversion of the Dap stereocenter to DDap, MDE3–119-7c, and substitution of His (MDE3–119-13c) also resulted in nanomolar antagonist potencies. The ligand containing Asn (MDE5–108-10c), representing the native loop sequence, was 3-fold less potent than MDE3–119-8c at the hMC4R, while the polar residue Ser (MDE3–85c) decreased potency 7-fold relative to MDE3–119-8c. The aliphatic Ala (MDE3–154c) and Abu (MDE3–119-2c) residues decreased antagonist potency 12-fold and 19-fold, respectively, compared to MDE3–119-8c, while the branched aliphatic Val (MDE3–119-10c) decreased potency 310-fold. Substitution of the acidic Glu (MDE3–119-5c) and Asp (MDE3–119-4c) amino acids decreased antagonist potency 70- and 90-fold, respectively, while the aromatic Phe substitution (MDE3–119-14c) decreased antagonist potency 80-fold. Comparing these data to a prior study at the mMC4R,[39] the ligands were equipotent at the human and mouse MC4R. Ranking compounds by antagonist potency resulted in the same order of ligands at the hMC4R and mMC4R, suggesting similar functional interactions at the two receptors. Several ligands also were shown to possess inverse agonist activity at the hMC4R, *vide infra*.

Binding Studies at the hMC4R:

In addition to functional potency, the ability of the macrocycles to displace radiolabeled ^{125}I-NDP-MSH and ^{125}I^{-}AGRP was studied in hMC4R-expressing HEK293 cells. Both NDP-MSH and AGRP utilize overlapping, but distinct binding sites on the MC4R.[47] Since the ligands in the present work were derived from the active loop of AGRP, it was hypothesized that the ligands might better occupy the binding site of AGRP, evident in greater displacement of ^{125}I-AGRP than ^{125}I-NDP-MSH. To examine this theory, both radiolabeled ligands were used.

Similar to previous studies, NDP-MSH displaced ^{125}I-NDP-MSH at 26 nM and AGRP displaced ^{125}I-AGRP at 12 nM concentrations (Table 1, Fig. 2a).[48–51] The macrocyclic peptides incorporating the native Asn (MDE5–108-10c) or the Dap substitution (MDE3–119-8c) were previously reported to displace ^{125}I-NDP-MSH, possessing IC_{50} values of 70

and 7.5 nM,[52] respectively, within a 3–4 fold range of the present report. As a general trend, the most potent AGRP-based macrocyclic ligands displaced the radiolabeled NDP-MSH and AGRP at the lowest concentrations, visualized in the linear correlation between pIC_{50} and pA_2 values (Fig. 2b). One compound, the Phe substituted MDE3–119-14c, possessed higher binding affinity than expected based upon the functional activity data (Fig. 2b, blue arrows). While there is a correlation between antagonist potency and binding affinity in the macrocyclic scaffold, the relatively increased affinity of MDE3–119-14c highlights the importance of characterizing functional antagonism and not rely on binding data to rank antagonist potency. The macrocyclic ligands were also observed to displace ^{125}I-AGRP at 2–3 fold lower concentrations compared to ^{125}I-NDP-MSH, supporting the hypothesis that the AGRP-derived ligands might better displace AGRP from the receptor binding pocket.

Inverse Agonism at the hMC4R:

Several macrocyclic ligands also possessed inverse agonist activity at the hMC4R (a sigmoidal dose-response curve demonstrating decreased signal from basal in at least two independent experiments, Fig. 3, Table 1). To quantify the inverse agonist activity, ligand dose-response curves were normalized to the response at 10^{-12} M concentrations, representing a basal signal for each ligand. The apparent potencies were determined from the inflection point of the normalized sigmoidal dose-response curves. The percent decrease from basal signal was determined from the average decrease from basal signal (signal at 10^{-12} M concentration) from replicates observed to possess a sigmoidal dose-response curve.

At the hMC4R, AGRP decreased the cAMP signal 35% from basal levels and possessed an apparent potency of 2.4 nM (Fig. 3, Table 1), similar to the observed antagonist potency. The apparent inverse agonist potencies followed a parallel trend to the antagonist pA_2 values, with the basic MDE3–119-8c, MDE3–119-7c, and MDE3–119-13c possessing nanomolar apparent inverse agonist potencies and variable decreases in cAMP signal (−50% for MDE3–119-8c, −30% for MDE3–119-7 and MDE3–119-13c). Similar apparent potencies (14 and 16 nM) and cAMP decreases (−30% and −25%) were observed for the polar Asn (MDE5–108-10c) and Ser (MDE3–85c, Fig 3) ligands. Substitution with Ala (MDE3–154c) or Abu (MDE3–119-2c; Fig. 3) resulted in apparent potencies of 50 and 22 nM and cAMP decreases of −35% and −15%, respectively. Macrocycles with acidic substitutions (MDE3–119-4c and MDE3–119-5c) possessed micromolar apparent potencies, and decreased cAMP (−35%) to the same extent as AGRP. Insertion of Phe (MDE3–119-14c) or Val (MDE3–119-10c; Fig. 3) resulted in ligands that did not possess an inverse agonist response at the hMC4R at up to 100 μM concentrations.

Generation, Characterization, and Pharmacology of D189 Mutant hMC4Rs:

Previously, a 3D GPCR homology molecular model of the hMC4R positioned the Asn114 side chain of AGRP in close proximity to the hMC4R D189 residue.[44] It was hypothesized that incorporating a basic residue into an AGRP-derived ligand at the Asn114 position may generate a new salt-bridge with the MC4R and increase antagonist potency,[38] supported by previous work at the mMC4R[38–39] and hMC4R (present study). Based upon the 2.8Å structure of the hMC4R with the synthetic SHU9119 peptide antagonist, the D189 hMC4R

residue is located on the second extracellular loop of the hMC4R.[53] The structure of the hMC4R co-crystalized with the synthetic antagonist SHU9119 ligand reports the hMC4R D189 side chain is angled toward, and is in proximity of the orthorsteric binding pocket of SHU9119.[53] These crystal structural data support the hypothesis that the hMC4R D189 residue is important for ligand binding and receptor function. To further probe for the potential for an AGRP-based ligand-hMC4R salt-bridge molecular interaction, a series of D189 mutant hMC4Rs were generated. Changing the D189 side chain moiety of the hMC4R to Glu (D189E) examined the consequence of extending the acidic side chain. The importance of the negative charge at the D189 position, while retaining a similarly sized side-chain, was examined by incorporating Asn (D189N) or Gln (D189Q). Another polar group, Ser (D189S) was also studied. The short, aliphatic Ala (D189A) was examined to remove charge and polar contacts. The basic Lys (D189K) examined the functional consequence of inverting the charge at this position. The mutant hMC4Rs were generated using standard polymerase chain reaction (PCR) based mutagenesis techniques, with a FLAG sequence (DYKDDDK) incorporated at the N-terminal.[54] Immunohistochemical cell expression studies using the FLAG sequence indicated that the total and cell surface expression of the six mutant receptors was similar to the wildtype hMC4R (Fig. 4).[54] These data indicate that these D189 hMC4R side chain modifications did not affect receptor cell surface expression or intracellular trafficking.

The D189 mutant hMC4Rs were characterized with a set of known agonists (α-MSH, NSP-MSH, MTII, and γ_2-MSH; Table 2 and Fig. 5). The four agonists were equipotent at the D189E, D189Q, and D189S hMC4Rs as compared to the wildtype hMC4R. At the D189N hMC4R, NDP-MSH maintained similar potency, with decreased potencies observed for α-MSH (170-fold), MTII (10-fold), and γ_2-MSH (35-fold), relative to the wildtype hMC4R. The D189A hMC4R possessed 500-, 28-, 90-, and 80-fold decreased potencies for α-MSH, NDP-MSH, MTII, and γ_2-MSH, respectively. These data differ from a previous publication reporting 1,400- and 3-fold decreased potencies for NDP-MSH and MTII at the D189A hMC4R using a CRE-luciferase cAMP assay.[55] Differences in the assays, receptor expression, and plasmid constructs may explain the potency variations reported herein and those observed in the previous report.[55] Decreased potencies of 230-, 10-, 21-, and 45-fold for α-MSH, NDP-MSH, MTII, and γ_2-MSH were observed at the D189K hMC4R. The binding affinities of I^{125}-NDP-MSH were within a two-fold range at the mutant hMC4 receptors (Table 3).

The mixed MC3R/MC4R antagonist, MC1R/MC5R agonist SHU9119[56] was assayed at the wildtype and D189 side chain modified hMC4Rs (Tables 2 & 4, Fig. 6). While the wildtype, D189E, D189N, D189S, D189A, and D189K hMC4Rs possessed minimal SHU9119-mediated cAMP stimulatory activity, the D189Q mutant was observed to possess partial agonist activity (25% maximal NDP-MSH signal, EC_{50} = 1.0 nM; Fig. 6) when stimulated by SHU9119. The antagonist potency of SHU9119 at the wildtype and mutant hMC4Rs were all within a 4-fold range (pA_2 values between 8.9 and 9.5), indicating the D189 position has minimal effects on SHU9119 functional potency.

The D189 mutant hMC4Rs were also characterized with AGRP (Tables 2 & 4, Fig. 7). AGRP was observed to possess inverse agonist activity at the D189E, D189N, D189Q, and

D189S hMC4Rs (Fig. 7). The magnitude of the inverse agonist response was strongest at the wildtype, D189E, and D189Q hMC4Rs, with a decreased response at the D189N and D189S hMC4Rs, and no apparent inverse agonist activity at the D189A or D189K hMC4Rs. When assayed at the D189E, D189N, D189Q and D189S hMC4Rs, AGRP possessed nanomolar antagonist potencies similar to the wildtype hMC4R. At the D189A and D189K hMC4Rs, AGRP potency decreased 80- and 40-fold, respectively. The observation that SHU9119 resulted in similar potency while a range was observed for AGRP at the hMC4R supports previous mMC4R mutagenesis data, indicating that these two ligands possess overlapping but distinct active sites.[47] The binding affinity of I^{125}-AGRP followed a similar trend to the observed antagonist potency (Table 3), with similar affinities at the wildtype, D189E, D189N, D189Q, and D189S hMC4Rs, 10-fold decreased affinity at D189K hMC4R and no affinity at concentrations up to 1 μM observed at the D189A hMC4R.

Nine of the AGRP-derived macrocyclic ligands were assayed at the D189 mutant hMC4Rs. The Val-substituted MDE3–119-10c was not assessed due to the low potency observed at the wildtype receptor and the Abu-substituted MDE3–119-2c was not assessed because it possessed similar pharmacology to the Ala-substituted MDE3–154c at the wildtype hMC4R. A similar trend for ligand potency was observed for the D189 mutant hMC4Rs as compared to the wildtype hMC4R. Basic substitutions (MDE3–119-8c, MDE3–119-7c, and MDE3–119-13c) were the most potent at the D189 hMC4Rs (Table 5, Fig. 8), which can be visualized by presenting the antagonist potency in radar plots (Fig. 9). Each spoke of the plot represents a hMC4R and the distance from the center of the graph indicates the potency at that receptor (higher potency is farther from the center). The plots for the basic-substituted macrocycles overlap AGRP, indicating similar antagonist potencies. Substituting polar (MDE5–108-10c, MDE3–85c) or short aliphatic (MDE3–119-154c) residues decreased potencies 4- to 30-fold compared to AGRP at the mutant receptors (Table 5), and results are plotted with the AGRP line (Fig. 9). Greater decreases (20- to 80-fold) were observed for the Phe substituted MDE3–119-14c, while the acidic Glu (MDE3–119-5c) or Asp (MDE3–119-4c) did not result in antagonist activity at the highest concentrations assayed (10, 5, 1, and 0.5 μM) at the D189A and D189K hMC4Rs.

These data suggest that the D189 hMC4R amino acid side chain is important for AGRP and AGRP-derived ligand binding and antagonist potency. However, it is not conclusive whether the D189 position forms an interaction with the Asn114 position of AGRP and the AGRP-derived macrocycles as previously hypothesized.[44] For macrocyclic ligands, basic substitutions at the AGRP-based Asn114 position resulted in the highest antagonist potency at the hMC4R. These basic substitutions possessed decreased potency at mutant hMC4Rs where the acidic D189 was changed to an uncharged Ala or basic Lys side chain, supporting the hypothesized interaction. However, a similar potency trend was observed for all macrocycles, regardless of the substitutions. Mutating the hMC4R to incorporate a basic residue (D189K) and substituting an acidic residue into the macrocyclic ligand (Asp/Glu [MDE3–119-4c/MDE3–119-5c]) did not recover antagonist potency. It should be noted that the 3D homology GPCR molecular model for the hMC4R and AGRP was generated using the C-terminal domain of AGRP (residues 87–132).[44] The present study involved cyclic peptides derived from the active loop of AGRP. In longer AGRP derivatives, other AGRP amino acids (outside the active loop and therefore not present in the current scaffold) may

position AGRP active loop residues with the hMC4R in orientations not possible in the macrocyclic scaffold. Alternatively, AGRP amino acids outside the active loop may create additional interactions with the hMC4R that modulate functional activity. Examining longer AGRP derivatives with acidic residue substitutions at the Asn114 position may be used in conjunction with D189K mutant hMC4Rs in future studies.

Inverse Agonism of AGRP and Macrocyclic Ligands at the D189 Mutant hMC4Rs:

Several AGRP-derived macrocyclic ligands possessed a variable inverse agonist activity response at the D189 modified hMC4Rs (Fig. 10, Table 6). The percent change from basal levels mirrored the pattern found in AGRP, with similar responses at the wildtype, D189E, and D189Q hMC4Rs, decreased responses for the D189S and D189N hMC4Rs, and no inverse agonist signal observed at the D189A and D189K hMC4Rs (Fig. 10, Table 6). One compound (MDE3–119-14c) did not possess inverse agonist activity at any of the hMC4Rs assayed, three (MDE3–119-13c, MDE3–154c, and MDE3–1194c) did not possess inverse agonist activity at the D189N hMC4R, and two (MDE3–119-13c, MDE3–154c) were not inverse agonists at the D189S hMC4R. Compounds possessed similar apparent potencies at the D189E hMC4R as compared to the wildtype receptor. At the D189N hMC4R, two ligands (MDE3–119-7c and MDE3–119-5c) were equipotent and four ligands (AGRP, MDE3–119-8c, MDE5–108-10c, and MDE3–85c) possessed decreased apparent potency compared to the wildtype receptor. Decreased apparent potencies (3- to 16-fold) were observed for most of the ligands at the D189Q hMC4R, as compared to the wildtype receptor, except for peptide MDE3–119-7c that was equipotent. At the D189S hMC4R, four ligands (MDE3–119-8c, MDE3–119-7c, MDE3–119-5c, and MDE3–119-4c) were equipotent compared to the wildtype receptor, while three (AGRP, MDE5–108-10c, and MDE3–85c) possessed 6- to 35-fold decreased apparent potencies.

As a general trend, compounds that possessed the highest inverse agonist apparent potencies at wildtype MC4R possessed similar apparent potencies at the D189 mutant hMC4Rs, similar to the trend observed for antagonist potencies at wildtype and mutant hMC4Rs. While many of the ligands possessed decreased apparent potencies at the D189N, D189Q, and D189S hMC4Rs as compared to the wildtype and D189E hMC4Rs, one ligand (MDE3–119-7c, DDap substitution) possessed equipotent nanomolar apparent potencies at all the hMC4Rs examined. Two ligands (MDE3–119-13c and MDE3–154c) did not possess inverse agonist activity at the D189N or at the D189S hMC4Rs, despite possessing sub-micromolar antagonist potencies at these receptors (MDE3–119-13c = 7.9 and 8.0, MDE3–154c = 7.1 and 7.2 at the D189N and D189S, respectively). The variable response at the mutant hMC4Rs indicates the D189 position may play an important role in the constitutive activity of the hMC4R, similar to that previously observed for mutants at the L250 position.[57] However, unlike the altered surface expression reported for the L250 mutations,[57] the D189 mutations did not alter the surface expression of the hMC4R (Figure 4).

Conclusions

Compounds that can modulate the MC4R may be therapeutic lead ligands that can be used to treat disease states of altered energy homeostasis. Herein, an AGRP-derived macrocyclic

scaffold previously shown to be equipotent to AGRP at the mMC4R was assayed for activity at the hMC4R, demonstrating similar antagonist potency between the mouse and human MC4Rs. The antagonist potency trend was similar to the trend in binding affinity and inverse agonist potency. A set of mutated hMC4Rs was generated to probe a postulated Asn114 (AGRP) and D189 (hMC4R) interaction. While these mutants minimally disrupted the synthetic SHU9119 MC4R antagonist activity, the D189 mutant hMC4Rs altered binding affinity, antagonist potency, and inverse agonist activity of AGRP and the AGRP-derived macrocyclic peptides. These data indicate that the D189 hMC4R position may provide a beneficial interaction with AGRP and AGRP-derived ligands that does not appear to be utilized in the SHU9119 ligand. This unique interaction may be exploited in the development of AGRP-derived ligands for modulating potency and efficacy at the MC4R in pursuing novel probe and therapeutic lead compounds for treating states of altered energy homeostasis.

Methods

Peptide Synthesis:

The coupling reagents [2-(1-H-benzotriazol-1-yl)-1,1,3,3-tetramethyluronium hexafluorophosphate (HBTU), benzotriazol-1-yl-oxy-tris(dimethylamino) phosphonium hexafluorophosphate (BOP), and 1-hydroxybenzotriazole (HOBt)], amino acids (unless otherwise noted), agouti-related protein (AGRP86–132), and the H-Pro-2-chlorotrityl resin were purchased from Peptides International (Louisville, KY). The Fmoc-DDap(Boc)-OH amino acid was purchased from Bachem (Torrance, CA). *N,N*-Dimethylformamide (DMF), dichloromethane (DCM), methanol, acetonitrile, and anhydrous ethyl ether were purchased from Fisher (Fair Lawn, NJ). Trifluoroacetic acid (TFA), dimethyl sulfoxide (DMSO), piperidine, and phenol were purchased from Sigma (St. Louis, MO). *N,N*-Diisopropylethylamine (DIEA) and triisopropylsilane (TIS) were purchased from Aldrich (Milwaukee, WI). All reagents and chemicals were ACS grade or better and were used without further purification.

The peptides were synthesized manually using standard Fmoc methodology[58] as previously described.[39] Briefly, the syntheses (0.05 mmol scale) consisted of the following steps on a preloaded H-Pro-2-chlorotrityl resin (0.68 mequiv/g substitution): (i) double-coupling of Fmoc-amino acid (3.1 equiv) with HBTU (3 equiv) and DIEA (5 equiv) in DMF for 1 h per coupling; (ii) removal of the *N*-Fmoc group by 20% piperidine in DMF (1 × 5 min, 1 × 20 min). Upon synthesis completion, peptides were cleaved from the resin with 1% TFA in DCM (v/v) for 6 min. The solution was concentrated and the protected peptides were precipitated and washed with cold (4 °C) diethyl ether. Cyclizations were performed overnight in DCM with a peptide concentration of 1 mg/mL using BOP (3 equiv), HOBt (3 equiv), and DIEA (6 equiv) to generate the amide bond between the Arg and Pro residues. The DCM was removed under reduced pressure, and the final side chain deprotection was performed in TFA:TIS:H_2O (95:2.5:2.5) for 2 h without further purification. Cyclic, deprotected peptides were precipitated and washed in cold diethyl ether.

All peptides were purified by RP-HPLC using a Shimadzu chromatography system with a photodiode array detector and a semi-preparative RP-HPLC C18 bonded silica column

(Vydac 218TP1010, 1.0 × 25 cm^2). The peptides were at least 95% pure as determined by analytical RP-HPLC in two diverse solvent systems and had the correct molecular mass by MALDI-MS (University of Minnesota Mass Spectrometry Lab).

Generation of D189 Mutants:

Receptor mutagenesis was performed as previously described.[47–49, 54] The human WT N-terminal FLAG-tagged MC4R cDNA (Supplemental Figure 1A) was generously provided by Dr. Robert Mackenzie[59] and was sub-cloned into the pBluescript plasmid (Stratagene) for subsequent mutagenesis. Site directed hMC4R mutagenesis was performed using a polymerase chain reaction (PCR) based strategy, using the Pfu turbo polymerase (Stratagene). Complementary sets of primers were designed containing nucleotide base pair changes resulting in the modified amino acids (Supplemental Figure 1B). Upon completion of the PCR reaction (95 ºC 30 s, 12 cycles of 95 ºC 30 s, 55 ºC 1 min, 68 ºC 9 min), the product was purified (Qiaquick PCR Purification Kit, Qiagen) and eluted in water. Subsequently, the sample was cut with *Dpn*1 (Invitrogen) to eliminate any methylated WT DNA, leaving only nicked circularized mutant DNA. The mutant hMC4R DNA was transformed into competent DH5α *E. coli* cells and single colonies were selected. The presence of the desired mutation was verified by DNA sequencing. The plasmid DNA containing the mutant was excised and sub-cloned into the *Hind*III/*Xba*I restrictions sites of the $pCDNA_3$ expression vector (Invitrogen). Complete FLAG-MC4R sequences were confirmed free of PCR nucleotide base errors by DNA sequencing (University of Florida sequencing core facilities).

Generation of Stable Cell Lines.

HEK-293 cells were maintained in Dulbecco's modified Eagle's medium (DMEM) with 10% fetal calf serum (FCS) and seeded 1 day prior to transfection at 1×10^6 cells/100-mm dish. Mutant and WT DNA in $pCDNA_3$ expression vector (20 μg) were transfected using the calcium phosphate method.[60] Stable receptor populations were generated using G418 selection (0.7–1 mg/mL) for subsequent bioassay analysis.

cAMP AlphaScreen® Bioassay:

Peptide ligands were dissolved in DMSO [NDP-MSH and AGRP(86–132) in H_2O] at a stock concentration of 10^{-2} M and were pharmacological characterized using the cAMP AlphaScreen® assay (PerkinElmer) according to the manufacturer's instructions and as previously described in the Haskell-Luevano laboratory.[61–63] Since the AlphaScreen cAMP assay is a loss-of-signal assay (decreased signal at higher concentrations), dose-response curves were normalized to NDP-MSH as previously described for illustrative purposes.[61, 64–65]

Briefly, cells 70–90% confluent were dislodged with Versene (Gibco®) at 37 °C and plated 10,000 cells/well in a 384-well plate (Optiplate™) with 10 μL freshly prepared stimulation buffer (1X HBSS, 5 mM HEPES, 0.5 mM IBMX, 0.1% BSA, pH = 7.4) with 0.5 μg anti-cAMP acceptor beads per well. The cells were stimulated with the addition of 5 μL stimulation buffer containing peptide (a seven point dose-response curve was used starting at

10^{-4} to 10^{-7} M, determined by ligand potency) or forskolin (10^{-4} M) and incubated in the dark at room temperature for 2 h.

Following stimulation, streptavidin donor beads (0.5 μg) and biotinylated-cAMP (0.62 μmol) were added to the wells in a subdued light environment with 10 μL lysis buffer (5 mM HEPES, 0.3% Tween-20, 0.1% BSA, pH = 7.4) and the plates were incubated in the dark at room temperature for an additional 2 h. Plates were read on a Enspire (PerkinElmer) Alpha-plate reader using a pre-normalized assay protocol (set by the manufacturer).

Data Analysis:

The EC_{50} and pA_2 values represent the mean of duplicate replicates performed in at least three independent experiments. The EC_{50} and pA_2 estimates and associated standard errors (SEM) were determined by fitting the data to a nonlinear least-squares analysis using the PRISM program (v4.0, GraphPad Inc.). The ligands were assayed as TFA salts and not corrected for peptide context.

Competitive Radioligand Binding Affinity Studies:

Human AGRP(86–132) and NDP-MSH were radiolabeled with $Na^{125}I$ using the chloramine-T method.[66] Monoradioiodinated peptide was purified from uniodinated and diradioiodinated peptide by HPLC, eluted isocratically using a mobile phase of acetonitrile and trimethylamine phosphate (pH 3.0).

Competitive binding assays were performed on HEK-293 cells stably expressing the wildtype and D189 modified hMC4Rs. Cells were plated 1–2 days before the experiment in 12-well tissue-culture plates (cat# 353043, Corning Life Sciences) and were grown to 90–100% confluency on the day of the assay. Media was gently aspirated and cells were treated with a freshly diluted aliquot of experimental non-labeled ligand at the appropriate concentration (a seven point dose-response curve starting at 10^{-4} to 10^{-6} M) in assay buffer (DMEM and 0.1% BSA) and a constant amount of ^{125}I-NDP-MSH or ^{125}I-AGRP(86–132) (100,000 cpm/well) for 1 h at 37 °C. The assay media was carefully aspirated and cells were washed once with assay buffer. Cell were lysed with 500 μL 0.1 M NaOH and 500 μL 1% Triton X-100 for a minimum of 10 min. The cell lysate was transferred to 12 × 75 mm polystyrene tubes (cat 14–961-13, Fisherbrand) and radioactivity quantified on a WIZARD^2 Automatic Gamma Counter (PerkinElmer). All experiments were performed with duplicate data points with at least two independent experimental replicates. The non-specific values were defined as a signal from 10^{-6} M unlabeled NDP-MSH or AGRP(86–132), corresponding to the respective ^{125}I-labeled peptide. Concentration-response curves and IC_{50} values were generated and analyzed by the PRISM program (version 4.0, GraphPad Inc.) by a nonlinear regression method. The standard error of the mean (SEM) was derived from the IC_{50} values from at least two independent experimental replicates.

Immunohistochemical Analysis of Wild type and D189 FLAG-Tagged hMC4Rs:

Flow cytometric analysis (FACS) of intracellular FLAG-tagged wild type hMC4R was performed as described previously.[48–49, 57] Briefly, cells were dissociated from monolayer culture dishes using cold Cell Dissociation buffer (Cellgro, Mediatech), centrifuged at 600xg

for 5min, room temperature, and the pelleted cells were resuspended in sterile-filtered FACS buffer (1% BSA, 0.1% Na azide, in 1xPBS pH 7.2; Sigma Chemical, St Louis MO). The cells were distributed to multiple FACS tubes (Falcon, Fisher Scientific) at one million cells per tube. The cells were treated with 10mg/mL unconjugated mouse IgG (Upstate Biotech or Sigma) to block nonspecific antibody binding. To determine cell surface receptor protein expression, the cells were then incubated for 45 min at room temperature with anti-FLAG-PE (Prozyme, San Leandro, CA). To determine the total cellular receptor protein expression, the cells were fixed with 2% methanol free formaldehyde in 1xPBS (Ted Pella or EM Scientific, Fisher Scientific) for 10min, permeabilized for 20 min with Saponin Buffer [0.5% saponin (Sigma) in FACS buffer, pH 7.2], and subsequently washed with Saponin Buffer. After centrifugation (600xg, 5min), cell aliquots were conjugated with anti-FLAG-APC antibodies (Prozyme) for 1h at room temperature to label the total (intracellular and surface) FLAG-tagged molecules. After the anti-FLAG antibody incubation, the labeled cells were washed 1mL of Saponin buffer 3 times prior to resuspension in FACS buffer for analysis. The PE- and APC-conjugated nonspecific antibodies (BD Biosciences-Pharmingen, CalTag, Burlingame, CA) served as isotype controls for the anti-FLAG antibody conjugates used in these analyses and were used to set the background for fluorescence staining detection on BD Biosciences FACS Calibur flow cytometers. Data were collected as both stained cell percentages (either surface or total detected) and as mean fluorescence per cell from a minimum of 10,000 collected events for each sample run. Receptor cell surface expression and total cellular expression (using permeabilized cells) were determined as summarized in Fig. 4 and were the results of at least three independent experiments.

Supplementary Material

Refer to Web version on PubMed Central for supplementary material.

Acknowledgements

This work has been supported by NIH Grants R01DK091906, R01DK057080, and R01DK064250, as well as by a 2017 Wallin Neuroscience Discovery Fund Award through the University of Minnesota. Mark D. Ericson was a recipient of an NIH Postdoctoral Fellowship (F32DK108402).

References

1. Smith PE, Experimental ablation of the hypophysis in the frog embryo. Science (1916), 44, 280–282. [PubMed: 17821767]
2. Allen BM, The results of extirpation of the anterior lobe of the hypophysis and of the thyroid of rana pipiens larvae. Science (1916), 44, 755–758. [PubMed: 17742316]
3. Haynes RC Jr.; Berthet L, Studies on the mechanism of action of the adrenocorticotropic hormone. J. Biol. Chem (1957), 225, 115–124. [PubMed: 13416222]
4. Huszar D; Lynch CA; Fairchild-Huntress V; Dunmore JH; Fang Q; Berkemeier LR; Gu W; Kesterson RA; Boston BA; Cone RD, et al., Targeted disruption of the melanocortin-4 receptor results in obesity in mice. Cell (1997), 88, 131–141. [PubMed: 9019399]
5. Chhajlani V; Muceniece R; Wikberg JE, Molecular cloning of a novel human melanocortin receptor. Biochem. Biophys. Res. Commun (1993), 195, 866–873. [PubMed: 8396929]
6. Chhajlani V; Wikberg JE, Molecular cloning and expression of the human melanocyte stimulating hormone receptor cDNA. FEBS Lett (1992), 309, 417–420. [PubMed: 1516719]

7. Chen C; Tucci FC; Jiang WL; Tran JA; Fleck BA; Hoare SR; Wen J; Chen TK; Johns M; Markison S, et al., Pharmacological and pharmacokinetic characterization of 2-piperazine-α-isopropyl benzylamine derivatives as melanocortin-4 receptor antagonists. Bioorg. Med. Chem (2008), 16, 5606–5618. [PubMed: 18417348]
8. Gantz I; Konda Y; Tashiro T; Shimoto Y; Miwa H; Munzert G; Watson SJ; DelValle J; Yamada T, Molecular cloning of a novel melanocortin receptor. J. Biol. Chem (1993), 268, 8246–8250. [PubMed: 8463333]
9. Gantz I; Miwa H; Konda Y; Shimoto Y; Tashiro T; Watson SJ; DelValle J; Yamada T, Molecular cloning, expression, and gene localization of a fourth melanocortin receptor. J. Biol. Chem (1993), 268, 15174–15179. [PubMed: 8392067]
10. Gantz I; Shimoto Y; Konda Y; Miwa H; Dickinson CJ; Yamada T, Molecular cloning, expression, and characterization of a fifth melanocortin receptor. Biochem. Biophys. Res. Commun (1994), 200, 1214–1220. [PubMed: 8185570]
11. Mountjoy KG; Robbins LS; Mortrud MT; Cone RD, The cloning of a family of genes that encode the melanocortin receptors. Science (1992), 257, 1248–1251. [PubMed: 1325670]
12. Roselli-Rehfuss L; Mountjoy KG; Robbins LS; Mortrud MT; Low MJ; Tatro JB; Entwistle ML; Simerly RB; Cone RD, Identification of a receptor for γ melanotropin and other proopiomelanocortin peptides in the hypothalamus and limbic system. Proc. Natl. Acad. Sci. U. S. A (1993), 90, 8856–8860. [PubMed: 8415620]
13. Griffon N; Mignon V; Facchinetti P; Diaz J; Schwartz JC; Sokoloff P, Molecular cloning and characterization of the rat fifth melanocortin receptor. Biochem. Biophys. Res. Commun (1994), 200, 1007–1014. [PubMed: 8179577]
14. Haynes RC, The activation of adrenal phosphorylase by the adreno-corticotropic hormone. J. Biol. Chem (1958), 233, 1220–1222. [PubMed: 13598765]
15. Nakanishi S; Inoue A; Kita T; Nakamura M; Chang AC; Cohen SN; Numa S, Nucleotide sequence of cloned cDNA for bovine corticotropin-β-lipotropin precursor. Nature (1979), 278, 423–427. [PubMed: 221818]
16. Bultman SJ; Michaud EJ; Woychik RP, Molecular characterization of the mouse agouti locus. Cell (1992), 71, 1195–1204. [PubMed: 1473152]
17. Lu D; Willard D; Patel IR; Kadwell S; Overton L; Kost T; Luther M; Chen W; Woychik RP; Wilkison WO, et al., Agouti protein is an antagonist of the melanocyte-stimulating-hormone receptor. Nature (1994), 371, 799–802. [PubMed: 7935841]
18. Miller MW; Duhl DM; Vrieling H; Cordes SP; Ollmann MM; Winkes BM; Barsh GS, Cloning of the mouse agouti gene predicts a secreted protein ubiquitously expressed in mice carrying the lethal yellow mutation. Genes Dev (1993), 7, 454–467. [PubMed: 8449404]
19. Ollmann MM; Wilson BD; Yang YK; Kerns JA; Chen YR; Gantz I; Barsh GS, Antagonism of central melanocortin receptors in vitro and in vivo by agouti-related protein. Science (1997), 278, 135–138. [PubMed: 9311920]
20. Fong TM; Mao C; MacNeil T; Kalyani R; Smith T; Weinberg D; Tota MR; VanderPloeg LHT, ART (protein product of agouti-related transcript) as an antagonist of MC-3 and MC-4 receptors. Biochem. Biophys. Res. Commun (1997), 237, 629–631. [PubMed: 9299416]
21. Shutter JR; Graham M; Kinsey AC; Scully S; Luthy R; Stark KL, Hypothalamic expression of ART, a novel gene related to agouti, is up-regulated in obese and diabetic mutant mice. Genes Dev (1997), 11, 593–602. [PubMed: 9119224]
22. Nijenhuis WAJ; Oosterom J; Adan RAH, AgRP(83–132) acts as an inverse agonist on the human-melanocortin-4 receptor. Mol. Endocrinol (2001), 15, 164–171. [PubMed: 11145747]
23. Haskell-Luevano C; Monck EK, Agouti-related protein functions as an inverse agonist at a constitutively active brain melanocortin-4 receptor. Regul. Pept (2001), 99, 1–7. [PubMed: 11257308]
24. Fan W; Boston BA; Kesterson RA; Hruby VJ; Cone RD, Role of melanocortinergic neurons in feeding and the agouti obesity syndrome. Nature (1997), 385, 165–168. [PubMed: 8990120]
25. Irani BG; Xiang ZM; Yarandi HN; Holder JR; Moore MC; Bauzo RM; Proneth B; Shaw AM; Millard WJ; Chambers JB, et al., Implication of the melanocortin-3 receptor in the regulation of food intake. Eur. J. Pharmacol (2011), 660, 80–87. [PubMed: 21199647]

26. Poggioli R; Vergoni AV; Bertolini A, ACTH-(1–24) and α-MSH antagonize feeding behavior stimulated by kappa opiate agonists. Peptides (1986), 7, 843–848. [PubMed: 3025825]
27. Brown KS; Gentry RM; Rowland NE, Central injection in rats of α-melanocyte-stimulating hormone analog: Effects on food intake and brain Fos. Regul. Pept (1998), 78, 89–94. [PubMed: 9879751]
28. Ebihara K; Ogawa Y; Katsuura G; Numata Y; Masuzaki H; Satoh N; Tamaki M; Yoshioka T; Hayase M; Matsuoka N, et al., Involvement of agouti-related protein, an endogenous antagonist of hypothalamic melanocortin receptor, in leptin action. Diabetes (1999), 48, 2028–2033. [PubMed: 10512369]
29. Farooqi IS; Keogh JM; Yeo GS; Lank EJ; Cheetham T; O'Rahilly S, Clinical spectrum of obesity and mutations in the melanocortin 4 receptor gene. N. Engl. J. Med (2003), 348, 1085–1095. [PubMed: 12646665]
30. Hinney A; Volckmar AL; Knoll N, Melanocortin-4 receptor in energy homeostasis and obesity pathogenesis. Prog. Mol. Biol. Transl. Sci (2013), 114, 147–191. [PubMed: 23317785]
31. Harris JI; Lerner AB, Amino-acid sequence of the α-melanocyte-stimulating hormone. Nature (1957), 179, 1346–1347. [PubMed: 13451616]
32. Creemers JW; Pritchard LE; Gyte A; Le Rouzic P; Meulemans S; Wardlaw SL; Zhu X; Steiner DF; Davies N; Armstrong D, et al., Agouti-related protein is posttranslationally cleaved by proprotein convertase 1 to generate agouti-related protein (AGRP)$_{83–132}$: Interaction between AGRP$_{83–132}$ and melanocortin receptors cannot be influenced by syndecan-3. Endocrinology (2006), 147, 1621–1631. [PubMed: 16384863]
33. Bolin KA; Anderson DJ; Trulson JA; Thompson DA; Wilken J; Kent SBH; Gantz I; Millhauser GL, NMR structure of a minimized human agouti related protein prepared by total chemical synthesis. FEBS Lett (1999), 451, 125–131. [PubMed: 10371151]
34. McNulty JC; Thompson DA; Bolin KA; Wilken J; Barsh GS; Millhauser GL, High-resolution NMR structure of the chemically-synthesized melanocortin receptor binding domain AGRP(87–132) of the agouti-related protein. Biochemistry (2001), 40, 15520–15527. [PubMed: 11747427]
35. Wilczynski A; Wang XS; Bauzo RM; Xiang Z; Shaw AM; Millard WJ; Richards NG; Edison AS; Haskell-Luevano C, Structural characterization and pharmacology of a potent (Cys101-Cys119, Cys110-Cys117) bicyclic agouti-related protein (AGRP) melanocortin receptor antagonist. J. Med. Chem (2004), 47, 5662–5673. [PubMed: 15509165]
36. Tota MR; Smith TS; Mao C; MacNeil T; Mosley RT; Van der Ploeg LHT; Fong TM, Molecular interaction of agouti protein and agouti-related protein with human melanocortin receptors. Biochemistry (1999), 38, 897–904. [PubMed: 9893984]
37. Joseph CG; Bauzo RM; Xiang ZM; Shaw AM; Millard WJ; Haskell-Luevano C, Elongation studies of the human agouti-related protein (AGRP) core decapeptide (Yc[CRFFNAFC]Y) results in antagonism at the mouse melanocortin-3 receptor. Peptides (2003), 24, 263–270. [PubMed: 12668211]
38. Ericson MD; Wilczynski A; Sorensen NB; Xiang ZM; Haskell-Luevano C, Discovery of a β-hairpin octapeptide, c[Pro-Arg-Phe-Phe-Dap-Ala-Phe-DPro], mimetic of agouti-related protein(87–132) [AGRP(87–132)] with equipotent mouse melanocortin-4 receptor (mMC4R) antagonist pharmacology. J. Med. Chem (2015), 58, 4638–4647. [PubMed: 25898270]
39. Ericson MD; Freeman KT; Schnell SM; Fleming KA; Haskell-Luevano C, Structure-activity relationship studies on a macrocyclic agouti-related protein (AGRP) scaffold reveal agouti signaling protein (ASP) residue substitutions maintain melanocortin-4 receptor antagonist potency and result in inverse agonist pharmacology at the melanocortin-5 receptor. J. Med. Chem (2017), 60, 8103–8114. [PubMed: 28813605]
40. Fleming KA; Ericson MD; Freeman KT; Adank DN; Lunzer MM; Wilber SL; Haskell-Luevano C, Structure-activity relationship studies of a macrocyclic AGRP-mimetic scaffold c[Pro-Arg-Phe-Phe-Asn-Ala-Phe-DPro] yield potent and selective melanocortin-4 receptor antagonists and melanocortin-5 receptor inverse agonists that increase food intake in mice. ACS Chem. Neurosci (2018), 9, 1141–1151. [PubMed: 29363944]
41. Ericson MD; Freeman KT; Haskell-Luevano C, Peptoid NPhe^4 in AGRP-based c[Pro^1-Arg^2-Phe^3-Phe^4-Xxx^5-Ala^6-Phe^7-DPro^8] scaffolds maintain mouse MC4R antagonist potency. ACS Med. Chem. Lett (2020), 11, 1942–1948. [PubMed: 33062177]

42. Fleming KA; Freeman KT; Ericson MD; Haskell-Luevano C, Synergistic multiresidue substitutions of a macrocyclic c[Pro-Arg-Phe-Phe-Asn-Ala-Phe-DPro] agouti-related protein (AGRP) scaffold yield potent and >600-fold MC4R versus MC3R selective melanocortin receptor antagonists. J. Med. Chem (2018), 61, 7729–7740. [PubMed: 30035543]
43. Ericson MD; Freeman KT; Schnell SM; Haskell-Luevano C, A macrocyclic agouti-related protein/[Nle^4,DPhe^7]α-melanocyte stimulating hormone chimeric scaffold produces subnanomolar melanocortin receptor ligands. J. Med. Chem (2017), 60, 805–813. [PubMed: 28045525]
44. Wilczynski A; Wang XS; Joseph CG; Xiang ZM; Bauzo RM; Scott JW; Sorensen NB; Shaw AM; Millard WJ; Richards NG, et al., Identification of putative agouti-related protein(87–132)-melanocortin-4 receptor interactions by homology molecular modeling and validation using chimeric peptide ligands. J. Med. Chem (2004), 47, 2194–2207. [PubMed: 15084118]
45. Joseph CG; Yao H; Scott JW; Sorensen NB; Marnane RN; Mountjoy KG; Haskell-Luevano C, γ_2-Melanocyte stimulation hormone (γ_2-MSH) truncation studies results in the cautionary note that γ_2-MSH is not selective for the mouse MC3R over the mouse MC5R. Peptides (2010), 31, 2304–2313. [PubMed: 20833220]
46. Schild HO, pA, a new scale for the measurement of drug antagonism. Br. J. Pharmacol (1947), 2, 189–206.
47. Haskell-Luevano C; Cone RD; Monck EK; Wan YP, Structure activity studies of the melanocortin-4 receptor by in vitro mutagenesis: Identification of agouti-related protein (AGRP), melanocortin agonist and synthetic peptide antagonist interaction determinants. Biochemistry (2001), 40, 6164–6179. [PubMed: 11352754]
48. Xiang ZM; Litherland SA; Sorensen NB; Proneth B; Wood MS; Shaw AM; Millard WJ; Haskell-Luevano C, Pharmacological characterization of 40 human melanocortin-4 receptor polymorphisms with the endogenous proopiomelanocortin-derived agonists and the agouti-related protein (AGRP) antagonist. Biochemistry (2006), 45, 7277–7288. [PubMed: 16752916]
49. Xiang ZM; Proneth B; Dirain ML; Litherland SA; Haskell-Luevano C, Pharmacological characterization of 30 human melanocortin-4 receptor polymorphisms with the endogenous proopiomelanocortin-derived agonists, synthetic agonists, and the endogenous agouti-related protein antagonist. Biochemistry (2010), 49, 4583–4600. [PubMed: 20462274]
50. Yang YK; Dickinson CJ; Zeng Q; Li JY; Thompson DA; Gantz I, Contribution of melanocortin receptor exoloops to agouti-related protein binding. J. Biol. Chem (1999), 274, 14100–14106. [PubMed: 10318826]
51. Yang YK; Thompson DA; Dickinson CJ; Wilken J; Barsh GS; Kent SBH; Gantz I, Characterization of agouti-related protein binding to melanocortin receptors. Mol. Endocrinol (1999), 13, 148–155. [PubMed: 9892020]
52. Koerperich ZM; Ericson MD; Freeman KT; Speth RC; Pogozheva ID; Mosberg HI; Haskell-Luevano C, Incorporation of agouti-related protein (AgRP) human single nucleotide polymorphisms (SNPs) in the AgRP-derived macrocyclic scaffold c[Pro-Arg-Phe-Phe-Asn-Ala-Phe-dPro] decreases melanocortin-4 receptor antagonist potency and results in the discovery of melanocortin-5 receptor antagonists. J. Med. Chem (2020), 63, 2194–2208. [PubMed: 31845801]
53. Yu J; Gimenez LE; Hernandez CC; Wu Y; Wein AH; Han GW; McClary K; Mittal SR; Burdsall K; Stauch B, et al., Determination of the melanocortin-4 receptor structure identifies Ca^{2+} as a cofactor for ligand binding. Science (2020), 368, 428–433. [PubMed: 32327598]
54. Haslach EM Rational drug design approaches targeting the mouse and human melanocortin receptors University of Florida, 2011.
55. Chapman KL; Kinsella GK; Cox A; Donnelly D; Findlay JB, Interactions of the melanocortin-4 receptor with the peptide agonist NDP-MSH. J. Mol. Biol (2010), 401, 433–450. [PubMed: 20600126]
56. Hruby VJ; Lu DS; Sharma SD; Castrucci AD; Kesterson RA; Al-Obeidi FA; Hadley ME; Cone RD, Cyclic lactam α-melanotropin analogs of Ac-Nle^4-cyclo[Asp^5,D-Phe^7,Lys^{10}] α-melanocyte-stimulating hormone-(4–10)-NH_2 with bulky aromatic amino acids at position 7 show high antagonist potency and selectivity at specific melanocortin receptors. J. Med. Chem (1995), 38, 3454–3461. [PubMed: 7658432]
57. Proneth B; Xiang ZM; Pogozheva ID; Litherland SA; Gorbatyuk OS; Shaw AM; Millard WJ; Mosberg HI; Haskell-Luevano C, Molecular mechanism of the constitutive activation of the

L250Q human melanocortin-4 receptor polymorphism. Chem. Biol. Drug Des (2006), 67, 215–229. [PubMed: 16611215]

58. Carpino LA; Han GY, 9-Fluorenylmethoxycarbonyl function, a new base-sensitive amino-protecting group. J. Am. Chem. Soc (1970), 92, 5748–5749.
59. Ho GY; MacKenzie RG, Functional characterization of mutations in melanocortin-4 receptor associated with human obesity. J. Biol. Chem (1999), 274, 35816–35822. [PubMed: 10585465]
60. Chen CA; Okayama H, Calcium phosphate-mediated gene transfer: a highly efficient transfection system for stably transforming cells with plasmid DNA. Biotechniques (1988), 6, 632–638. [PubMed: 3273409]
61. Ericson MD; Schnell SM; Freeman KT; Haskell-Luevano C, A fragment of the *Escherichia coli* ClpB heat-shock protein is a micromolar melanocortin 1 receptor agonist. Bioorg. Med. Chem. Lett (2015), 25, 5306–5308. [PubMed: 26433448]
62. Singh A; Tala SR; Flores V; Freeman K; Haskell-Luevano C, Synthesis and pharmacology of α/β^3-peptides based on the melanocortin agonist Ac-His-DPhe-Arg-Trp-NH_2 sequence. ACS Med. Chem. Lett (2015), 6, 568–572. [PubMed: 26005535]
63. Tala SR; Schnell SM; Haskell-Luevano C, Microwave-assisted solid-phase synthesis of side-chain to side-chain lactam-bridge cyclic peptides. Bioorg. Med. Chem. Lett (2015), 25, 5708–5711. [PubMed: 26555357]
64. Lensing CJ; Freeman KT; Schnell SM; Adank DN; Speth RC; Haskell-Luevano C, An in vitro and in vivo investigation of bivalent ligands that display preferential binding and functional activity for different melanocortin receptor homodimers. J. Med. Chem (2016), 59, 3112–3128. [PubMed: 26959173]
65. Elster L; Elling C; Heding A, Bioluminescence resonance energy transfer as a screening assay: Focus on partial and inverse agonism. J. Biomol. Screening (2007), 12, 41–49.
66. Hunter WM; Greenwood FC, Preparation of iodine-131 labelled human growth hormone of high specific activity. Nature (1962), 194, 495–496. [PubMed: 14450081]
67. Jackson PJ; McNulty JC; Yang YK; Thompson DA; Chai BX; Gantz I; Barsh GS; Millhauser GL, Design, pharmacology, and NMR structure of a minimized cystine knot with agouti-related protein activity. Biochemistry (2002), 41, 7565–7572. [PubMed: 12056887]

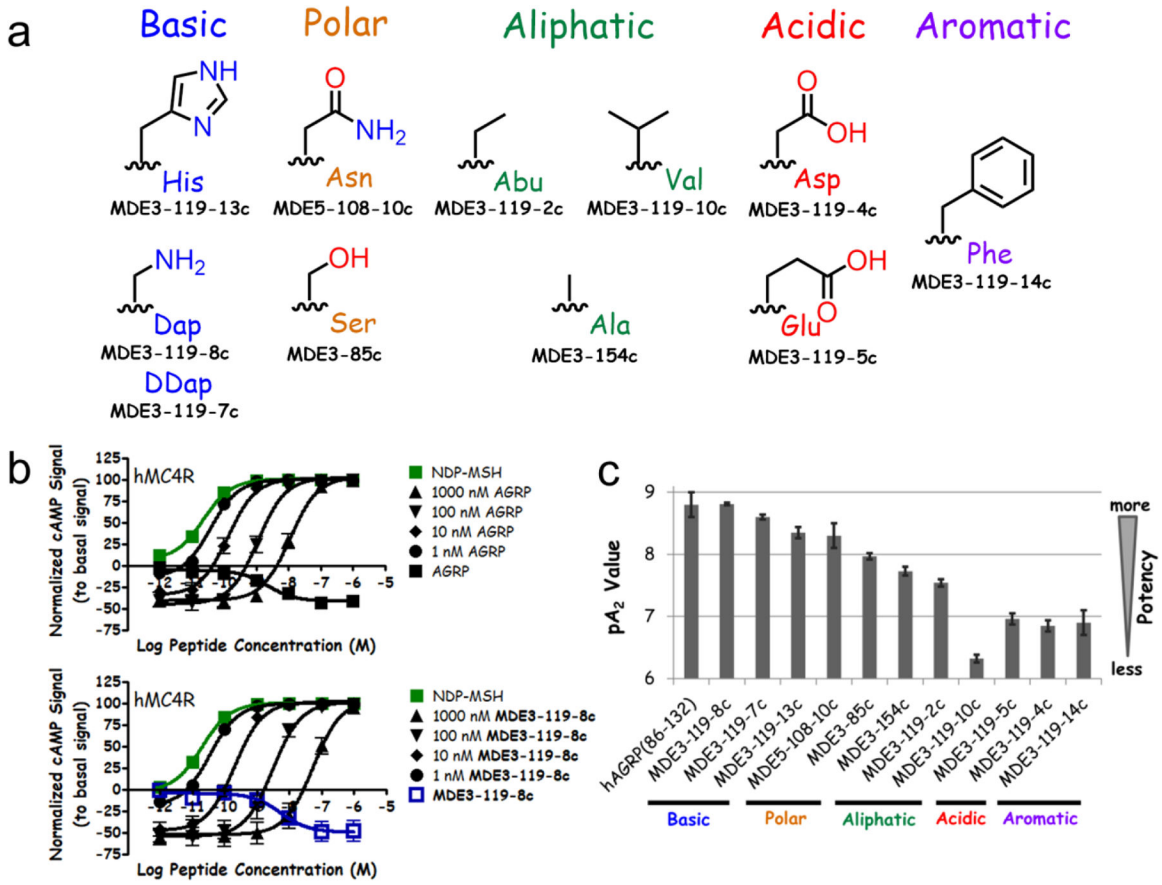

Figure 1:

(a) Structures of the amino acid side chains and corresponding compound numbers. (b) Illustration of the antagonist and inverse agonist pharmacology for hAGRP(86–132) and MDE3–119-8c at the hMC4R. SEM error bars are plotted, but may be smaller than the symbol representation. (c) Antagonist potencies (pA_2 values) of ligands at the hMC4R. Error bars are SEM.

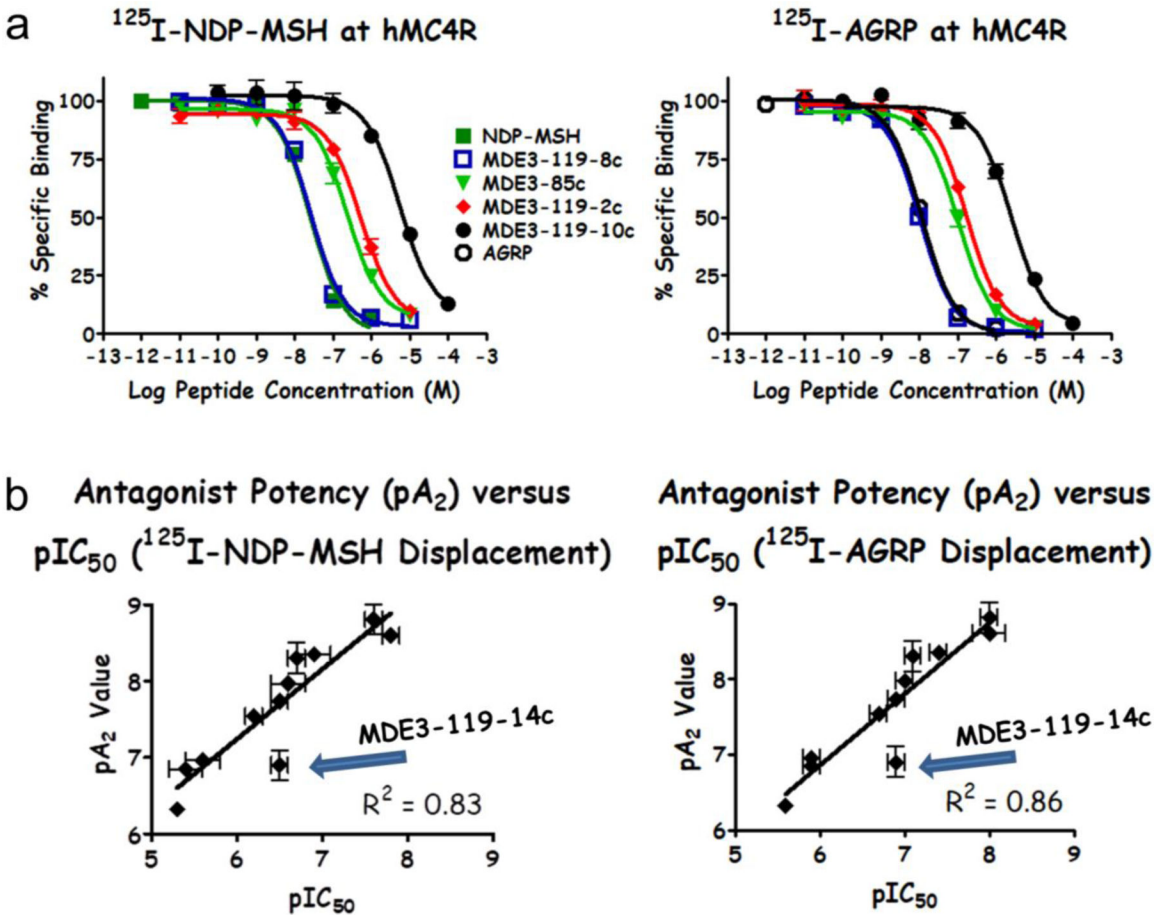

Figure 2:

(a) Illustration of radiolabeled displacement curves for NDP-MSH, AGRP, MDE3–119-8c, MDE3–85c, MDE3–119-2c, and MDE3–119-10c at the hMC4R. (b) Correlation of pIC_{50} (displacing ^{125}I-NDP-MSH or ^{125}I-AGRP) values versus pA_2 values for AGRP-derived macrocyclic ligands at the hMC4R. The blue arrows indicate ligand MDE3–119-14c.

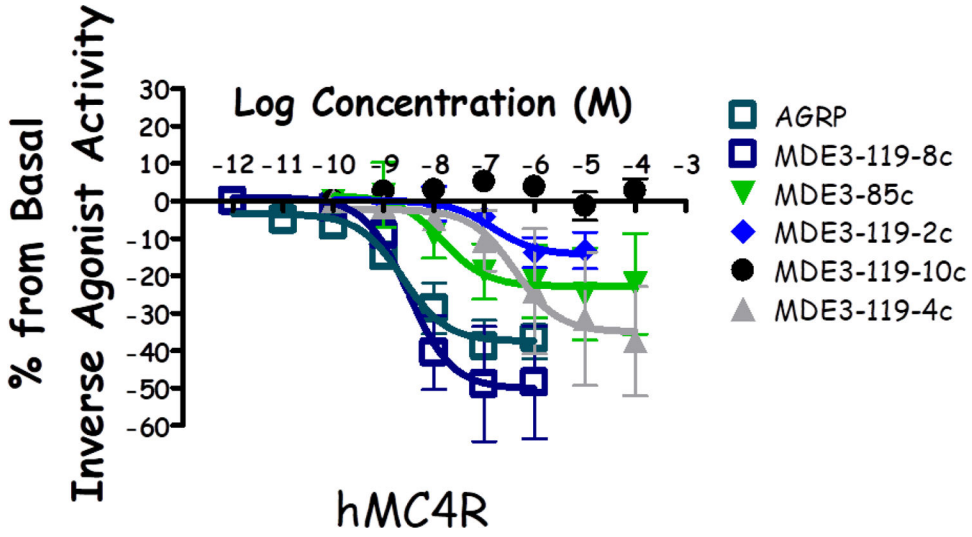

Figure 3:
Illustration of the inverse agonist pharmacology for select ligands at the hMC4R.

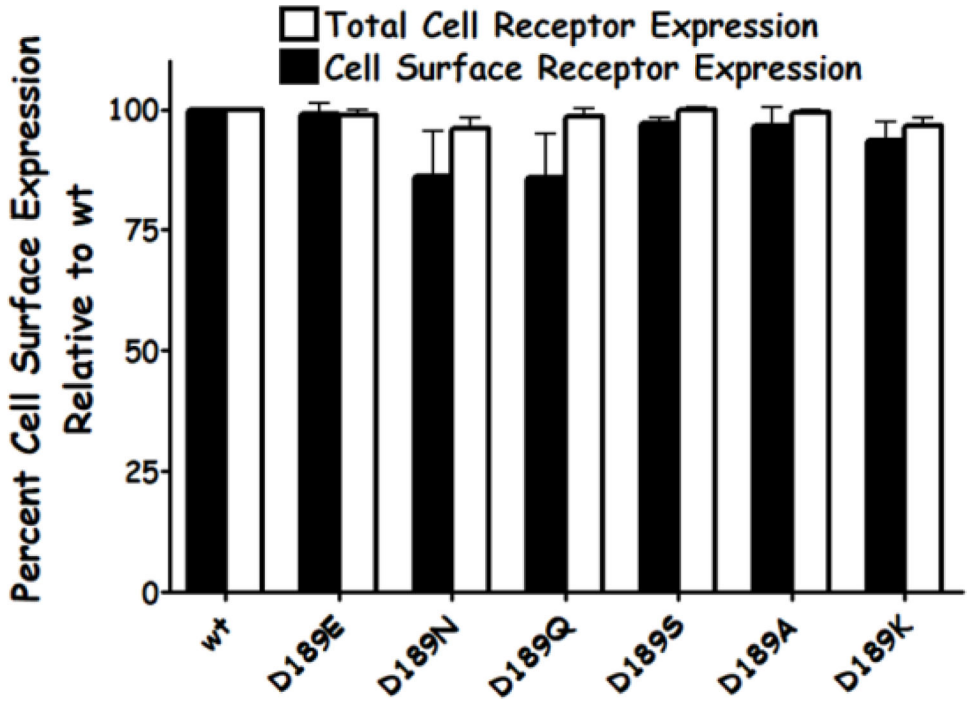

Figure 4:

Fluorescence-activated cell sorting (FACS) analysis of the WT and D189 mutant hMC4Rs in stably expressing HEK-293 cells. The total cell receptor expression levels were determined using permeabilized cells measuring both cell surface and intracellular protein expression. The cell surface expression levels were determined using nonpermeabilized cells. Expression levels are presented relative to the WT hMC4R control. These are the average of at least 3 independent experiments.

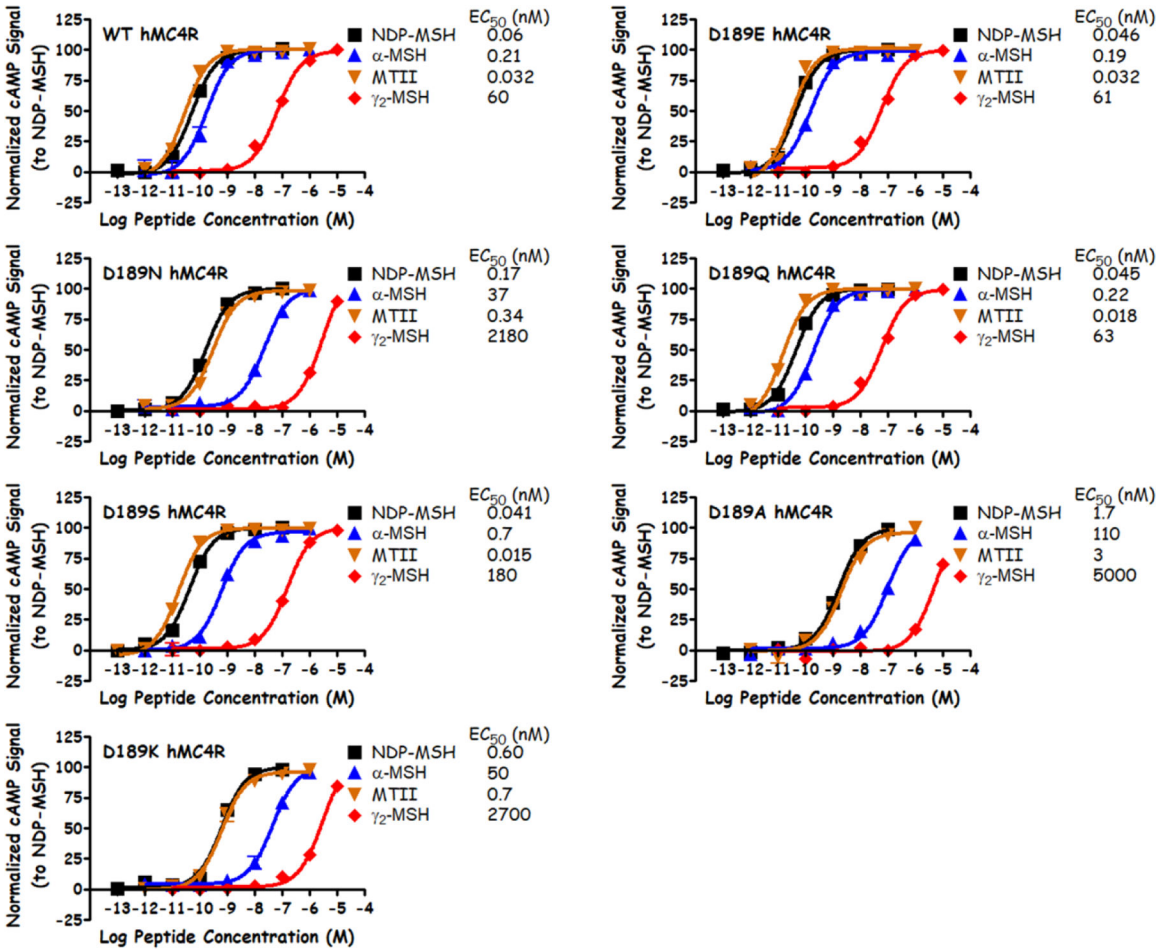

Figure 5:

Illustration of the agonist pharmacology for ligands α-MSH, NDP-MSH, MTII and γ_2-MSH at the WT and D189 hMC4Rs. SEM error bars are plotted, but may be smaller than the symbol representation.

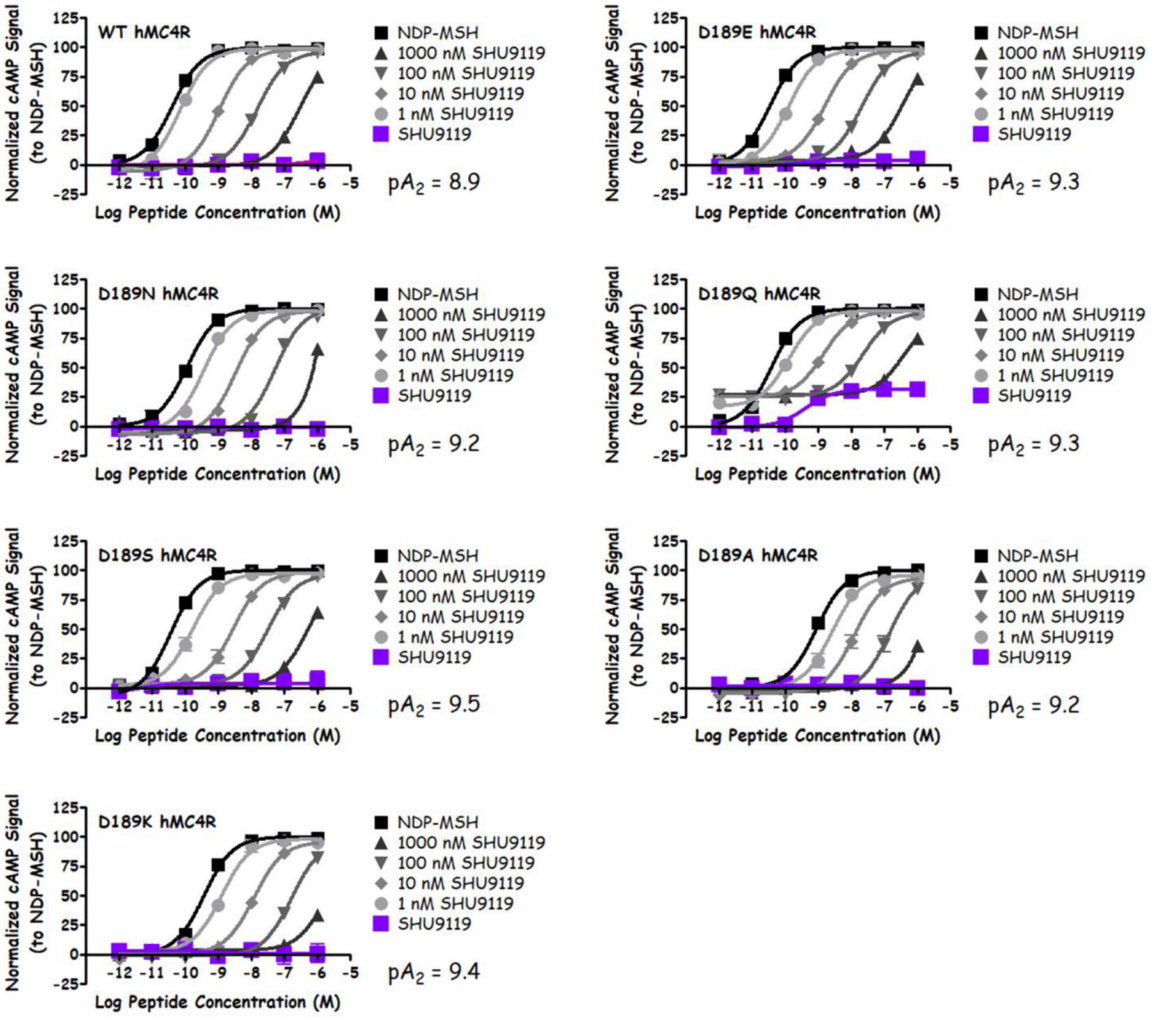

Figure 6:

Illustration of SHU9119 antagonist pharmacology at the WT and D189 mutant hMC4Rs. SEM error bars are plotted, but may be smaller than the symbol representation.

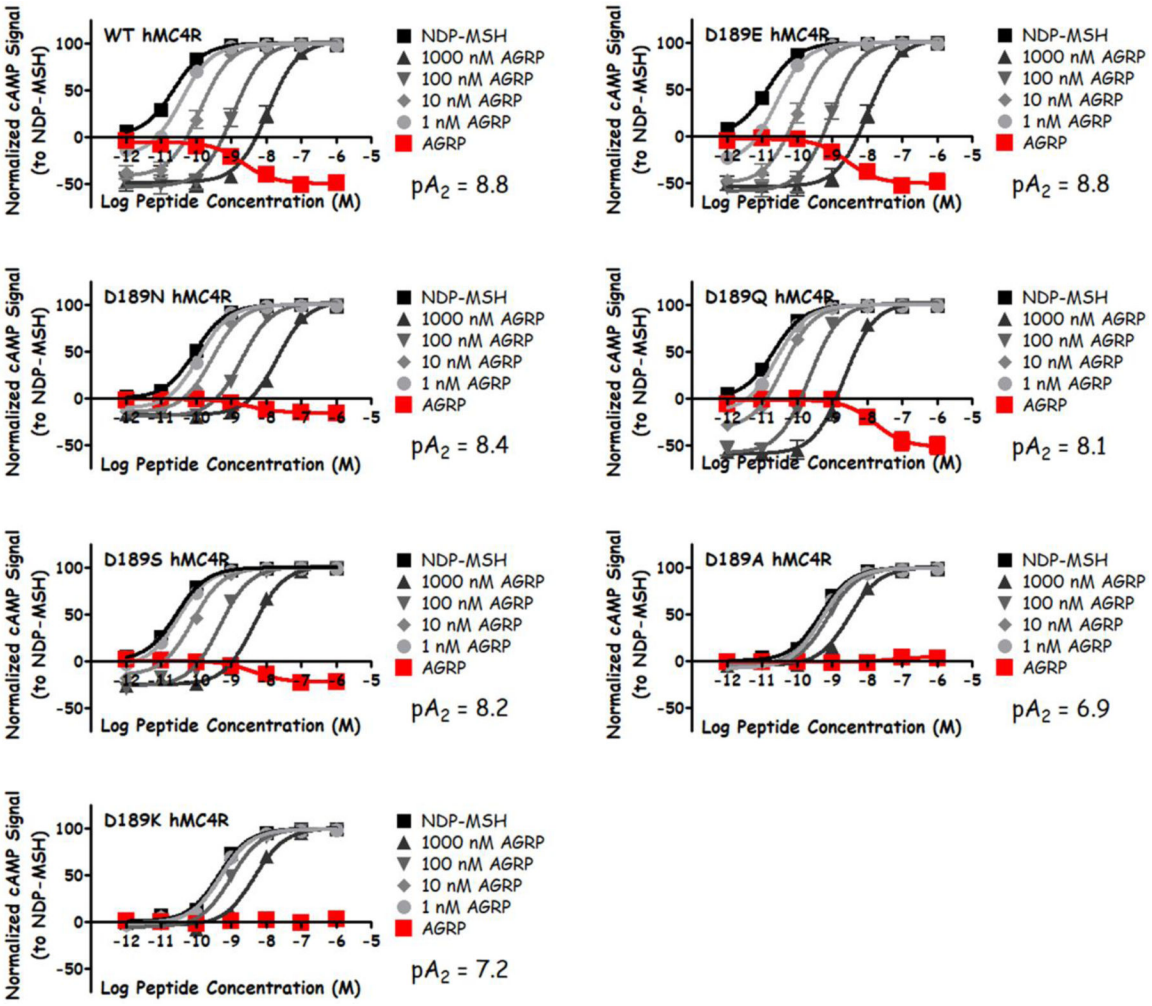

Figure 7:

Illustration of AGRP antagonist and inverse agonist pharmacologies at the WT and D189 mutant hMC4Rs. SEM error bars are plotted, but may be smaller than the symbol representation.

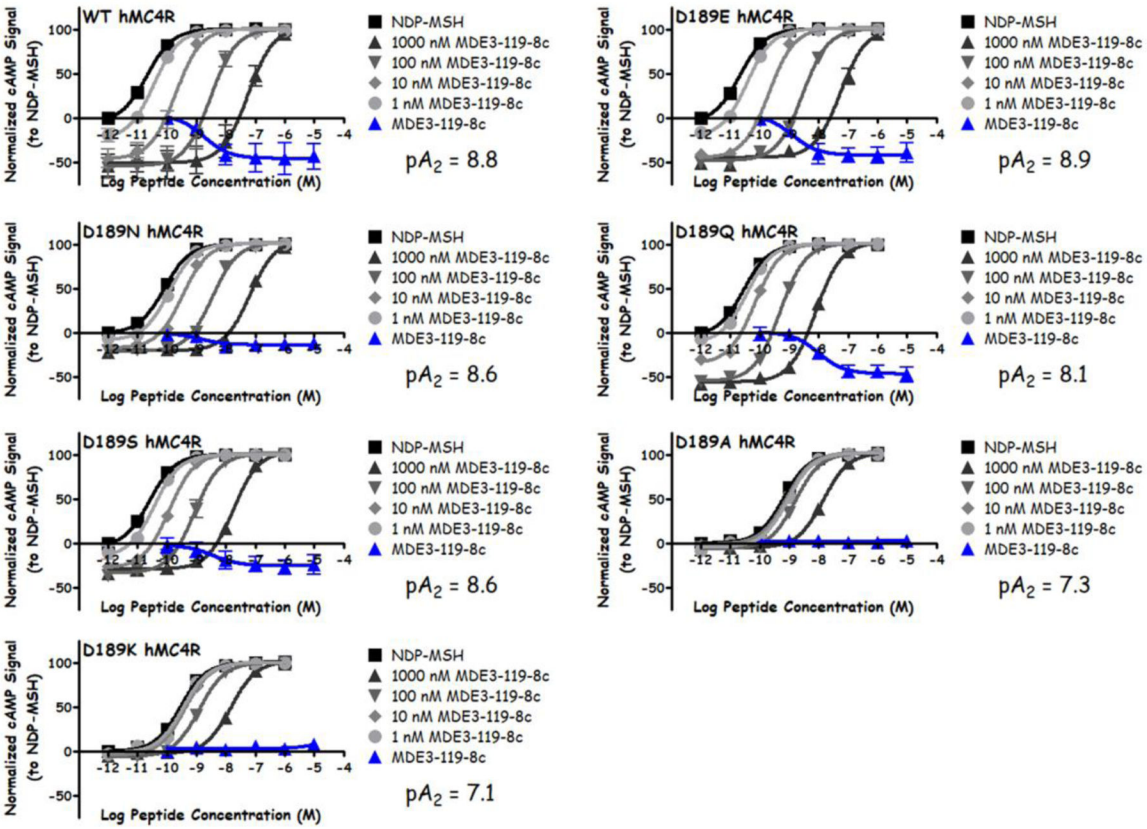

Figure 8:

Illustration of MDE3–119-8c antagonist and inverse agonist pharmacologies at the WT and D189 mutant hMC4Rs. SEM error bars are plotted, but may be smaller than the symbol representation.

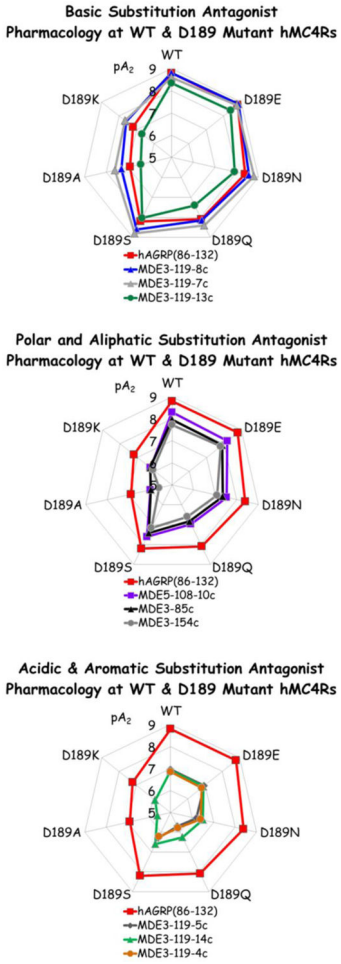

Figure 9:

Summary of the antagonist pharmacology at WT and D189 mutant hMC4Rs graphed as radar plots. Each spoke of a radar plot represents the indicated hMC4R. Data are plotted as pA_2 values ascending outward (the more potent the compound, the further it resides from the center of the graph). If pA_2 values could not be determined (MDE3–119-4c and MDE3–119-5c at the D189A and D189K hMC4Rs), no data are graphed. The compounds are presented in three groups: (1) basic substitutions within the macrocyclic scaffold (Dap, MDE3–119-8c; D-Dap, MDE3–119-7c; His, MDE3–119-13c), (2) polar and aliphatic substitutions within the macrocyclic scaffold (Asn, MDE5–108-10c; Ser, MDE3–85c; Ala, MDE3–154c), and (3) acidic and aromatic substitutions within the macrocyclic scaffold (Glu, MDE3–119-5c; Phe, MDE3–119-14c; Asp, MDE3–119-4c). In each graph, AGRP is included for reference (red squares).

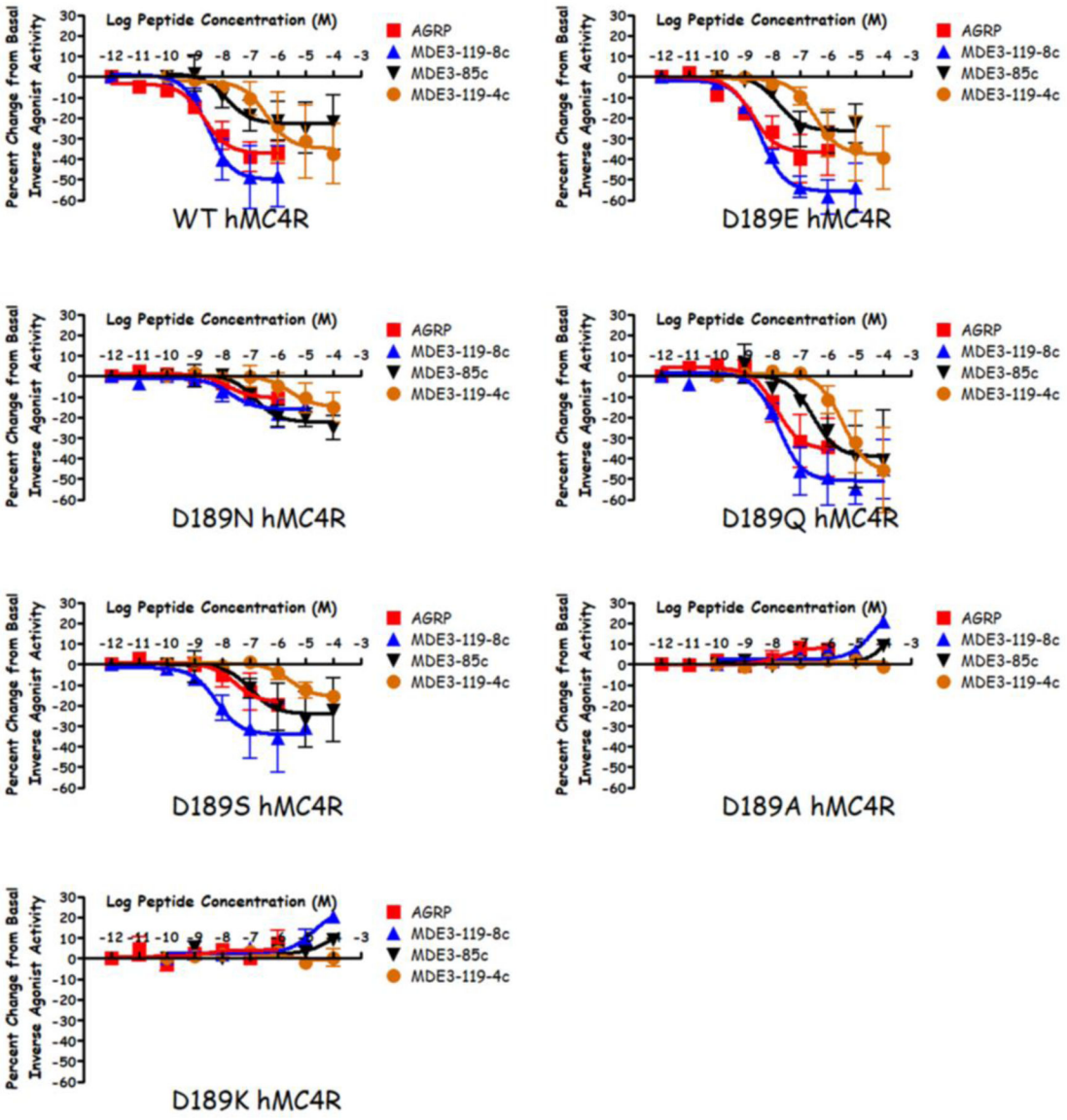

Figure 10:

Illustration of the inverse agonist pharmacology of AGRP, MDE3–119-8c, MDE3–85c, and MDE3–119-4c at the WT and D189 mutant hMC4Rs.

Table 1:

Peptide Antagonist Pharmacology, Inverse Agonist Activity, and Binding Affinity at the Human Melanocortin-4 Receptor.[a]

Peptide	Sequence	hMC4R			
		Antagonist	Inverse Agonist	^{125}I-NDP-MSH	^{125}I-AGRP
		pA_2	EC_{50} (nM)	IC_{50} (nM)	
hAGRP(86–132)		8.8±0.2	2.4±0.5 (−35%)	11±1[b]	12±1
MDE5–108-10c	c[Pro-Arg-Phe-Phe-*Asn*-Ala-Phe-DPro]	8.3±0.2	14±3 (−30%)	200±30	78±6
MDE3–119-8c	c[Pro-Arg-Phe-Phe-*Dap*-Ala-Phe-DPro]	8.8±0.1	3.4±1.9 (−50%)	26±1	11±1
MDE3–119-7c	c[Pro-Arg-Phe-Phe-*DDap*-Ala-Phe-DPro]	8.6±0.1	4±2 (−30%)	16±1	11±4
MDE3–119-13c	c[Pro-Arg-Phe-Phe-*His*-Ala-Phe-DPro]	8.4±0.1	8±6 (−30%)	120±50	44±7
MDE3–85c	c[Pro-Arg-Phe-Phe-*Ser*-Ala-Phe-DPro]	8.0±0.1	16±4 (−25%)	260±90	110±20
MDE3–154c	c[Pro-Arg-Phe-Phe-*Ala*-Ala-Phe-DPro]	7.7±0.1	50±20 (−35%)	340±40	120±10
MDE3–119-2c	c[Pro-Arg-Phe-Phe-*Abu*-Ala-Phe-DPro]	7.5±0.1	22±8 (−15%)	600±200	190±20
MDE3–119-5c	c[Pro-Arg-Phe-Phe-*Glu*-Ala-Phe-DPro]	7.0±0.1	1,100±800 (−35%)	2,500±900	1,400±200
MDE3–119-14c	c[Pro-Arg-Phe-Phe-*Phe*-Ala-Phe-DPro]	6.9±0.2	none	320±50	115±5
MDE3–119-4c	c[Pro-Arg-Phe-Phe-*Asp*-Ala-Phe-DPro]	6.8±0.1	2,000±1,000 (−35%)	3,600±1,300	1,300±100
MDE3–119-10c	c[Pro-Arg-Phe-Phe-*Val*-Ala-Phe-DPro]	6.3±0.1	none	5,400±1,500	2,400±600

[a]The indicated errors represent the standard error of the mean determined from at least two (binding) or three (antagonist/inverse agonist pharmacology) independent experiments. The antagonistic pA_2 values were determined using the Schild analysis and the agonist NDP-MSH. None indicates that no inverse agonist activity was observed. The percent for inverse agonist activity indicates the decrease from basal signal for the ligand.

[b]The displacement of ^{125}I-NDP-MSH by AGRP(87–132) was previously reported by Jackson *et al.*[67]

Table 2:

Agonist Activity of Control Melanocortin Ligands at the Wild-type and D189 Mutant hMC4Rs.[a]

Peptide	EC_{50} (nM)						
	WT	**D189E**	**D189N**	**D189Q**	**D189S**	**D189A**	**D189K**
α-MSH	0.21±0.07	0.19±0.03	37±8	0.22±0.03	0.7±0.2	110±20	50±10
NDP-MSH	0.06±0.01	0.046±0.007	0.17±0.04	0.045±0.005	0.041±0.007	1.7±0.4	0.60±0.02
MTII	0.032±0.004	0.032±0.008	0.34±0.06	0.018±0.001	0.015±0.003	3±1	0.7±0.2
γ_2-MSH	60±20	61±6	2,180±90	63±8	180±20	5,000±2,000	2,700±200
SHU9119	>100,000	>100,000	>100,000	Partial Agonist 1.0±0.4 nM (25% NDP-MSH)	>100,000	>100,000	>100,000
AGRP(86–132)	Inverse Agonist	Inverse Agonist	Inverse Agonist	Inverse Agonist	Inverse Agonist	>100,000	>100,000

[a]The indicated errors represent the standard error of the mean determined from at least three independent experiments. >100,000 indicates that the control peptide did not possess agonist activity at concentrations up to 100 μM. Partial agonist indicates that the peptide resulted in sub-maximal receptor activation, with the indicated apparent EC_{50} value and percent maximal NDP-MSH stimulation. Inverse Agonist indicates that the peptide possessed inverse agonist activity at the receptor (EC_{50} values and percent deviation from basal are reported in Table 6).

Table 3:

Binding Affinities of Control Melanocortin Ligands at the Wild-type and D189 Mutant hMC4Rs.[a]

Peptide	Binding IC_{50} (nM)						
	WT	**D189E**	**D189N**	**D189Q**	**D189S**	**D189A**	**D189K**
NDP-MSH/I^{125}-NDP-MSH[b]	10 ± 1	17 ± 5	17 ± 3	10 ± 2	8.9 ± 0.1	13.4 ±0.7	17 ± 4
AGRP(86–132)/I^{125}-AGRP(86–132)	12 ± 2	6 ± 1	10.5 ± 0.7	10 ± 1	12.5 ± 0.7	>1000	150 ± 60

[a]The indicated errors represent the standard deviation determined from two independent experiments. >1000 indicates that an IC_{50} could not be determined up to 1 μM concentrations.

[b]The values for NDP-MSH/I^{125}-NDP-MSH were previously reported by Haslach.[54]

Table 4:

Antagonist Activity of Control Melanocortin Ligands at the Wild-type and D189 Mutant hMC4Rs.[a]

Peptide	pA_2						
	WT	**D189E**	**D189N**	**D189Q**	**D189S**	**D189A**	**D189K**
SHU9119	8.9±0.1	9.3±0.1	9.2±0.1	9.3±0.1	9.5±0.2	9.2±0.1	9.4±0.1
AGRP(86–132)	8.8±0.2	8.8±0.1	8.4±0.1	8.1±0.1	8.2±0.8	6.9±0.1	7.2±0.2

[a]The indicated errors represent the standard error of the mean determined from three independent experiments. The antagonistic pA_2 values were determined using the Schild analysis and the agonist NDP-MSH.

Table 5:

Peptide Antagonist (pA_2) Pharmacology at Human WT and D189 Mutant Melanocortin-4 Receptors.[a]

Peptide	Sequence	WT	D189E	D189N	D189Q	D189S	D189A	D189K
hAGRP(86–132)		8.8±0.2	8.8±0.1	8.4±0.1	8.1±0.1	8.2±0.2	6.9±0.1	7.2±0.2
MDE5–108-10c	c[Pro-Arg-Phe-Phe-*Asn*-Ala-Phe-DPro]	8.3±0.2	8.2±0.1	7.5±0.1	7.0±0.1	7.6±0.1	6.0±0.1	6.3±0.1
MDE3–119-8c	c[Pro-Arg-Phe-Phe-*Dap*-Ala-Phe-DPro]	8.8±0.1	8.9±0.1	8.6±0.1	8.1±0.1	8.6±0.2	7.3±0.1	7.6±0.1
MDE3–119-7c	c[Pro-Arg-Phe-Phe-*DDap*-Ala-Phe-DPro]	8.6±0.1	8.8±0.1	8.8±0.1	8.4±0.2	8.8±0.1	7.6±0.1	7.7±0.1
MDE3–119-13c	c[Pro-Arg-Phe-Phe-*His*-Ala-Phe-DPro]	8.4±0.1	8.4±0.1	7.9±0.1	7.4±0.1	8.0±0.1	6.4±0.1	6.7±0.1
MDE3–85c	c[Pro-Arg-Phe-Phe-*Ser*-Ala-Phe-DPro]	8.0±0.1	7.9±0.1	7.4±0.1	6.8±0.1	7.4±0.1	6.0±0.1	6.3±0.1
MDE3–154c	c[Pro-Arg-Phe-Phe-*Ala*-Ala-Phe-DPro]	7.7±0.1	7.8±0.1	7.1±0.1	6.6±0.1	7.2±0.1	5.6±0.1	6.1±0.1
MDE3–119-5c	c[Pro-Arg-Phe-Phe-*Glu*-Ala-Phe-DPro]	7.0±0.1	6.9±0.1	6.2±0.1	5.7±0.1	6.3±0.1	<5.5	<5.5
MDE3–119-14c	c[Pro-Arg-Phe-Phe-*Phe*-Ala-Phe-DPro]	6.9±0.2	6.9±0.1	6.5±0.1	6.2±0.1	6.6±0.2	5.6±0.1	5.9±0.1
MDE3–119-4c	c[Pro-Arg-Phe-Phe-*Asp*-Ala-Phe-DPro]	6.8±0.1	6.8±0.1	6.4±0.1	5.8±0.1	6.2±0.1	<5.5	<5.5

[a]The indicated errors represent the standard error of the mean determined from at least three independent experiments. The antagonistic pA_2 values were determined using the Schild analysis and the agonist NDP-MSH. ND indicates the values were not determined. The use of <5.5 indicates that no antagonist activity was observed at the highest assayed concentrations (10,000, 5,000, 1,000, and 500 nM).

Table 6:

Peptide Inverse Agonist Pharmacology at the Human WT and D189 Mutant Melanocortin-4 Receptors.[a]

Peptide	Sequence	WT	D189E	D189N	D189Q	D189S
hAGRP(86–132)		2.4±0.5 (−35%)	4.4±0.1 (−35%)	30±10 (−10%)	17±5 (−35%)	20±10 (−20%)
MDE5–108-10c	c[Pro-Arg-Phe-Phe-*Asn*-Ala-Phe-DPro]	14±3 (−30%)	11.6±0.6 (−25%)	100±60 (−20%)	123±3 (−45%)	80±40 (−20%)
MDE3–119-8c	c[Pro-Arg-Phe-Phe-*Dap*-Ala-Phe-DPro]	3.4±1.9 (−50%)	3.4±2.2 (−55%)	190±188 (−15%)	16±8 (−45%)	8±5 (−35%)
MDE3–119-7c	c[Pro-Arg-Phe-Phe-*DDap*-Ala-Phe-DPro]	4±2 (−30%)	4±2 (−35%)	10±2 (−15%)	9±4 (−40%)	14±8 (−30%)
MDE3–119-13c	c[Pro-Arg-Phe-Phe-*His*-Ala-Phe-DPro]	8±6 (−30%)	13±5 (−15%)	none	32±8 (−30%)	none
MDE3–85c	c[Pro-Arg-Phe-Phe-*Ser*-Ala-Phe-DPro]	16±4 (−25%)	11±4 (−25%)	100±40 (−20%)	250±150 (−35%)	600±400 (−25%)
MDE3–154c	c[Pro-Arg-Phe-Phe-*Ala*-Ala-Phe-DPro]	50±20 (−35%)	16±2 (−25%)	none	170±40 (−25%)	none
MDE3–119-5c	c[Pro-Arg-Phe-Phe-*Glu*-Ala-Phe-DPro]	1,100±800 (−35%)	1,100±900 (−40%)	3,000±2,000 (−5%)	7,000±2,000 (−40%)	1,600±200 (−20%)
MDE3–119-14c	c[Pro-Arg-Phe-Phe-*Phe*-Ala-Phe-DPro]	none	none	none	none	none
MDE3–119-4c	c[Pro-Arg-Phe-Phe-*Asp*-Ala-Phe-DPro]	2,000±1,000 (−35%)	3,000±2,000 (−40%)	none	7,000±5,000 (−45%)	6,000±3,000 (−15%)

[a]The indicated values represent the apparent inverse agonist potencies (inflection point of the sigmoidal dose-response curve). The reported errors represent the standard error of the mean determined from at least two independent experiments. The percentage represents the percent decrease from basal activity observed. None indicates that inverse agonist activity was not observed in at least two experimental replicates.